# Lumped parameter modelling of a thermoelectric cooler for high power electronics

# Lumped parameter modelling of a thermoelectric cooler for high power electronics

**G Casano[1] and S Piva[1]**

[1] DE Department of Engineering, Università di Ferrara, Ferrara, Italy
Corresponding author e-mail: stefano.piva @unife.it

**Abstract.** A detailed analysis based on a lumped parameter model is presented of a cooling system for electronic equipments based on the combination of Peltier cells, air-cooling and liquid cold plate. A comprehensive model, specifically tailored for the cooling system under investigation, is introduced; the whole set of assumptions useful for the description of each element of the lumped parameter model, is described in depth. The model has been calibrated through an exhaustive comparison of numerical results versus experimental data, based on data gathered in experiments already published. Despite the large number of simplifying assumptions, the general good accordance between calculated and measured results demonstrate the reliability of the lumped parameter model, intended to be used for predicting the behaviour of the cooling system for currently untestable experimental conditions. Finally, the model is used as a useful design tool to investigate the cooling circuit under different operating conditions, in order to optimise the cooling solution here proposed.

## 1. Introduction

Nowadays, in power electronics, high efficiency, small size and low weight are required. High efficiency means, among others, compactness and low cooling power demand. However, as usual in power electronics, compactness frees spaces, and makes them available for an extra power production. For larger power the heat release is large again and thus efficient cooling systems are needed to avoid overheating. It is well known that an excessive temperature increase means a shorten expected life of the components, in particular a degradation in the insulation of the windings in the coils, an increase of the core losses in the inductors, a degradation of the dielectrics in capacitors, a shorter life of the active components, like MOSFETs.

In power electronics, power supply systems belong to a sector showing a continuous development. In recent years, this evolution has been motivated by the need of the best conversion efficiency, the reason why the SMPSs (Switch Mode Power Supplies) were born. An SMPS, like any other power supply unit, transfers energy to a direct current (DC) load from a source in direct current (DC) or alternating current (AC), converting its current and voltage characteristics. Applications of the SMPSs are many, especially for low powers. The examples of utilizations of the SMPSs for high power are fewer (for instance an application in the power supply of RF amplifiers for digital television transmission [1]).

An innovative field, which offers many possibilities for the use of SMPS converters / power supplies in high power applications, is automotive. For example, to be able to accumulate the energy taken from the electric network (AC), in a battery (DC) placed on an electric vehicle (EV), SMPSs are used [2,3]. SMPSs are also used bi-directionally (acceleration and braking) in electric vehicles (EVs) and hybrid electric vehicles (HEVs) [3,4].

As already discussed in [1,5], in a SMPS converter the most overheated components are usually the passive ones (condensers, coils, transformers). In this situation liquid cooling, usually considered an efficient and reliable cooling solution in high power utilizations, present difficulties in cooling the cumbersome passive components. While it is easy to place the active components directly on a liquid cold plate, the large passive components of a SMPS (capacitors, transformers and coils) need to be placed on a printed circuit board (PCB). It is difficult with a cold plate to maintain both PCB and passive components at the design temperature, because the latter are originally developed for air-cooling. For this reason, we developed a hybrid solution, using both liquid- and air-cooling [1,5].
In details, we produce an airflow, for cooling the passive components, with a large finned surface, in its turn cooled by a cold plate. Finally, the cooling liquid is refrigerated with a low-cost external heat exchanger. The solutions presented in [1] and in [5] differ for the presence of Peltier cells between the finned heat sink and the cold plate. These cells are necessary to get an airflow temperature lower than the ambient temperature. Gupta et al. [6] tested a similar solution for a high frequency on-board electric vehicle charger. They also proposed [6] a different solution, consisting in the encapsulation in a thermal potting epoxy of the magnetic components (transformers and coils). Heat is transferred to the cold plate through heat pipes.
For the liquid cooled Switch-Mode Power Supply (SMPS) discussed in [5], the results are presented of a theoretical investigation on its thermal behaviour. The analysis is based on a lumped parameter model of the cooling system. Lumped parameter models are largely used in engineering for their simplified mathematical and numerical approaches, which minimises the necessity for computationally intensive procedures. Their fields of application are very different: thermal plants [7,8], heat pipes [9], geothermal plants [10], electrical machines [11], blood flow in systemic arteries [13].
A comprehensive model, specifically tailored for the cooling system under investigation, is thus introduced; the whole set of assumptions useful for the description of each element of the lumped parameter model, is described in depth. The model has been validated through an exhaustive comparison of numerical results versus experimental data, based on data gathered in experiments already published [5]. Despite the large number of simplificative assumptions, the general good accordance between calculated and measured results demonstrate the reliability of the lumped parameter model, intended to be used for predicting the behaviour of the cooling system for currently untestable conditions. Finally, the model is used as a useful design tool to investigate the cooling circuit under different operating conditions, in order to optimise the cooling solution here proposed.

## 2. Model and Calibration

The cooling solution proposed in [5] is here modelled with a system of non-linear equations based on energy balance equations made on the different sub-systems of the equipment:

- PCB and components.
- internal air,
- finned heat sink,
- Peltier cells refrigerator,
- cold-plate,
- air-cooled radiator.

In figure 1 a lumped parameter model of the cooling system based on an equivalent electric scheme is shown.
Heat is produced on the PCB principally by the passive components (coils, condensers and transformers), since the active components are placed directly on the cold plate [5].
The energy balance for the passive components is given by:

$$Q_a = \frac{T_{pc} - T_{a,i}}{R_{pc}} \tag{1}$$

where $Q_a$ is the heat dissipated by the electronic components as a function of efficiency and of power absorbed by the electronic system.
The thermal power to be cooled in the finned heat sink is given by:

$$Q_C = Q_a + Q_{fan} + Q_{diss} \tag{2}$$

In more details, $Q_{diss}$ is given by:

$$Q_{diss} = (KS)_{a,m-e}(T_e - T_{a,m}) + (KS)_{w,m-a,m}(T_{w,m} - T_{a,m}) + (KS)_{a,i-e}(T_e - T_{a,i}) \tag{3}$$

where the different terms $(KS)_i$ in figure 1 are indicated in form of thermal resistance as $R_i$.
The energy balance of the finned heat sink is given by:

$$R_f Q_C = \frac{(T_{a,i} - T_C) - (T_{a,o} - T_C)}{\ln \frac{(T_{a,i} - T_C)}{(T_{a,o} - T_C)}} \tag{4}$$

$$-Q_C = (\rho c)_{a,o} Q_{v,a} (T_{a,i} - T_{a,o}) \tag{5}$$

The energy balance in the Peltier cells cooling system is given by:

$$R_c Q_C = N(T_C - T_c) \tag{6}$$

$$Q_C = N\left[S_{cell} I_{cell} T_c - 0.5 R_{el,cell} I_{cell}^2 - K_{cell}(T_h - T_c)\right] \tag{7}$$

$$Q_H = -(Q_C + N V_{cell} I_{cell}) \tag{8}$$

$$R_h Q_H = N(T_{w,m} - T_h) \tag{9}$$

$$V_{cell} = (T_h - T_c) S_{cell} + R_{cell} I_{cell} \tag{10}$$

where $S_{cell}$, $R_{el,\,cell}$ and $K_{cell}$ are the parameters characterizing the Peltier cells.
The energy balance in the cold plate is given by:

$$Q_w = Q_H + Q_{MOSFET} + (Q_{diss})_{e-w,m} - (Q_{diss})_{a,m-w,m} \tag{11}$$

where the terms $(Q_{diss})_i$ are the contributions to the heat exchanged by the cold plate with the ambient.
The energy balance in the radiator is given by:

$$-Q_w = (\rho c)_{w,m} Q_{v,w} (T_{w,o} - T_{w,i}) \tag{12}$$

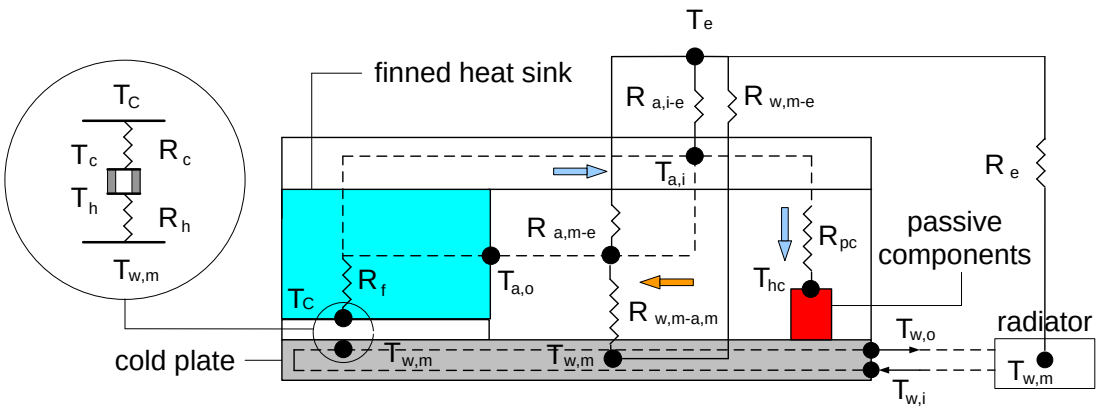


**Figure 1.** Lumped parameter schematics of the cooling system.

$$Q_w = \frac{T_{w,m} - T_e}{R_e} \tag{13}$$

With equations (1-13) we are able to arrange a set on nonlinear equations, consisting of a system of 9 equations with 9 unknowns: $T_{pc}$, $T_{w,i}$, $T_{w,o}$, $T_C$, $T_{a,i}$, $T_{a,o}$, $T_h$, $T_c$ and I.
This system is solved iteratively with a freezing procedure, where at each pass just one equation and one unknown are considered. The remaining unknowns are "known" with the value pertaining to the previous pass.
The parameters characterizing the Peltier cells are obtained on the base of their data sheet, by following the method proposed in [13]. The Peltier cells originally used in the experiment [5] were chosen of rectangular shape (50 × 25 mm), so as to overlap the pipes of the cold plate, with a limited protrusion over the plate. The main characteristics of the commercial BiTe-based Peltier cells (Kryotherm TB-195-1.0-0.8) are $I_{max}$ = 5.8 A, $V_{max}$ = 24.1 V, $Q_{max}$ = 86 W, $\Delta T_{max}$ = 68 K, at a reference temperature $T_h$ = 300 K. Furthermore, the factor form of the thermoelements is $G = 1.25 \cdot 10^{-3}$ m, since their area is $A = 10^{-6}$ m$^2$ and the thickness $L = 8 \cdot 10^{-4}$ m.
Preliminarily, in the tuning operations, the thermal resistances $R_e$, $R_f$ and $R_{pc}$ are interpolated on the base of the available experimental data; their expressions are:

$$R_e(T_{w,m}) = \sum_{i=1}^{5} a_i (T_{w,m})^{i-1} \tag{14}$$

$$R_f(T_C) = \sum_{i=1}^{2} a_i (T_C)^{i-1} \tag{15}$$

$$R_{pc}(T_{a,i}) = \sum_{i=1}^{2} a_i (T_{a,i})^{i-1} \tag{16}$$

Successively, the different $(KS)_i$ included in equation (3) are tuned, with a regression routine, on the base of the already available experimental data for the seven unknowns of the model, reported in [5]. The tuning operation is considered concluded when the calculated values of the unknowns agree with the experimental ones. In figure 2 calculated values of the unknowns and the corresponding experimental values, grouped in two graphs for the different scales, are compared, in order to show the final agreement and the quality of the tuning operation.
Furthermore, in table 1 a comparison of calculated and experimental values of power, more specifically cooling power, $Q_C$, water to air power $Q_w$ and power absorbed by the Peltier cells, $Q_{TEC}$, is shown. As for the unknown parameters of figure 2, also in the comparison of table 1 a very good agreement is confirmed.

## 3. Results

The model proposed in Paragraph 2 has been used to scale up our integrated air-water cooling system for values of useful power, $Q_{DL}$, higher than those experimented in [5]. For practical reasons, in [5] the maximum useful power supplied was of 3 kW. In the future it will be possible that this useful power could be increased up to $Q_{DL}$ = 5 kW. With our model, based on the available experimental data, it will be possible to individuate solutions useful to guarantee the exercise requirements, in particular an acceptable temperature for passive and active components, also for the heaviest operating conditions. It will be also interesting an analysis of the exercise conditions for values of the ambient parameters lower than the upper limits normally used in the design step.
The design parameters are $T_{a,i}$ = 30°C and $T_e$ = 40°C. This value of ambient temperature, $T_e$, is accepted by several recognized standards. For instance, in [14] this is the upper limit for the extreme operating conditions of the equipment and the requirements shall be met with the equipment operated at this value. The cooling air temperature, $T_{a,i}$, is chosen so that for the airflow flow rate, the highest temperature of the passive components will be lower than 90°C.

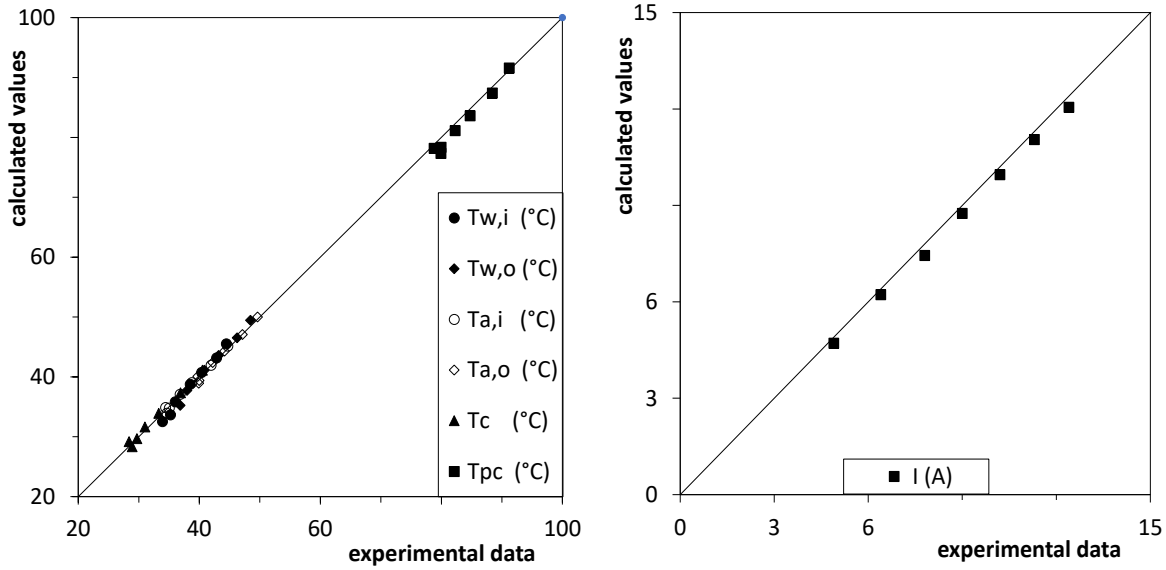


**Figure 2.** Comparison between experimental data and calculated values after the tuning process of the main parameters used in the mathematical model of the cooling system.

**Table 1.** Comparison of experimental and calculated values of power.

| $Q_C$ (W) | | $Q_w$ (W) | | $Q_{TEC}$ (W) | |
|---|---|---|---|---|---|
| exp. | calc. | exp. | calc. | exp. | calc. |
| 76.41 | 71.72 | 269.2 | 257.5 | 87.02 | 83.73 |
| 80.49 | 76.75 | 332.6 | 321.6 | 152.0 | 147.8 |
| 81.18 | 79.20 | 402.6 | 387.0 | 226.0 | 215.6 |
| 81.87 | 80.46 | 480.3 | 476.5 | 315.4 | 306.7 |
| 81.35 | 79.40 | 578.5 | 573.6 | 417.1 | 407.1 |
| 77.93 | 76.96 | 696.1 | 679.9 | 528.6 | 516.9 |
| 73.73 | 72.65 | 819.5 | 792.8 | 653.4 | 635.1 |

As design constrains, we use as fixed conditions some of the parameters measured in [5]. In more details, water and air mass flow rates are: $Q_{v,a}$ = 43.0 $m^3$/h, $Q_{v,w}$ = 0.176 $m^3$/h.
Width and height of the finned heat sink are also kept constant, while the length is increased or decreased with the number of the Peltier cells. The thermal resistance of the finned heat sink is then increased or decreased as a function of the length of the fins.
The total number of cells is subdivided in modules of equal number of cells. Inside the modules the cells are electrically connected in series. In the whole cooling system, the modules are then wired in parallel.
The unknown parameters of the design exercise are the number of cells, N, and the voltage of the thermoelectric cooler, V.
As the main design requirement, we chose a high value of the Energy Efficiency Ratio (EER) of the thermoelectric cooling system, so to reduce the electricity consumption. EER is defined by:

$$\mathrm{EER} = \frac{Q_C}{Q_{TEC}} \tag{17}$$

In figure 3 the distributions of EER are shown as a function of the number of Peltier cells and for

different values of useful power, $Q_{DL}$. The whole set of distributions of EER show a maximum, more evident for low powers, $Q_{DL}$. For an assigned value of $Q_C$, the highest the EER, the lowest the energy consumption of the Peltier cells. Therefore, in EER distributions it is possible to identify an optimal number of cells, N, for each useful power value, $Q_{DL}$, able to assure the design condition with the minimum energy consumption. It is also evident that for the maximum useful power considered, $Q_{DL}$ = 5 kW, the maximum is not clearly recognizable.
In figure 3, the cooling power, $Q_C$, is also shown. This value is definitely independent on the number of cells.
By combining EER and $Q_C$, the absence of a clear maximum means that for the highest values of $Q_{DL}$, the number of cells is not significant in terms of energy consumption. For these values of $Q_{DL}$, the choice will move from the optimum value of N, to the minimum able to assure the design requirements. In this way for the same costs of exercise, the minimum initial cost will be guaranteed.
Afterwards, we studied in deep the trends of the EER shown in figure 3, by putting in evidence all the contributions to equation (17). Through equation (7), the cooling power, $Q_C$, can be unbundled in three different contributions: Peltier, Joule and Fourier. The cooling power is a linear combination of these three terms.
In figure 4 the cooling power, $Q_C$, is shown together with the power absorbed by the Peltier cells, $Q_{TEC}$. Furthermore, the power of the three terms Peltier, Joule and Fourier is also shown. The whole set of values is graphed as a function of the total number of cells. The results refer to $Q_{DL}$ = 5 kW.
The thermoelectric effect is mainly due to a balance between Peltier and Fourier terms. The role played by the Joule term is always lower. Necessarily, the Peltier term increases with the number of cells, while the Fourier one decreases.
While $Q_C$ is quite constant with the number of cells (figure 3), the power absorbed by the cells, $Q_{TEC}$, reflecting the Peltier term, increases. $Q_{TEC}$ shows a minimum, even if barely outlined because of the scale of the axes, in correspondence of N = 116. This is the same number of cells already seen in figure 3.
In figure 5 the design number of cells is shown as a function of the useful power, $Q_{DL}$. The "maximum EER" number of cells increases quadratically with $Q_{DL}$, because this is the trend shown by the electric power dissipated by the power supply, $Q_a$ [1], which is the main contribution to $Q_C$. In figure 5 the trend of the cooling power per single cell, $Q_C/N$, is also shown. This parameter is quite constant, with a slight tendency to a linear increase with the useful power. This is due to the dependency on the

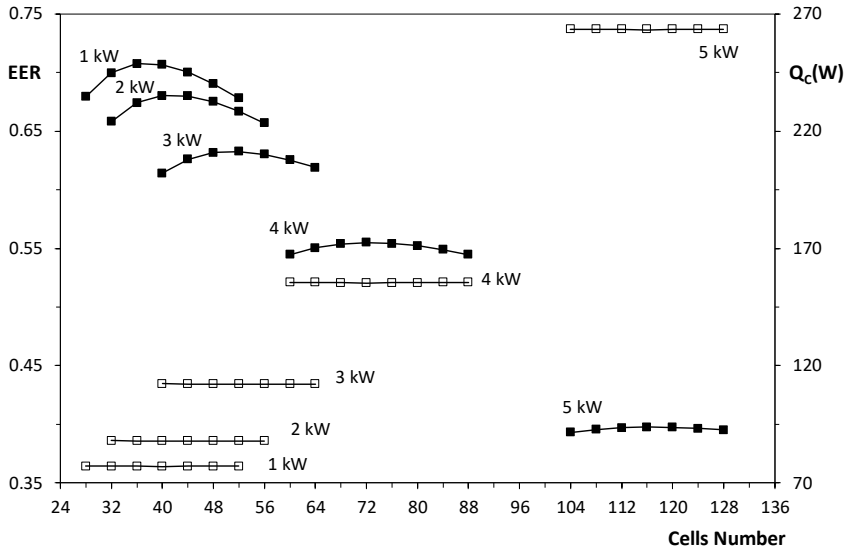


**Figure 3.** Distributions of EER (black symbols) and $Q_C$ (white symbols) as a function of the number of cells and for different values of useful power.

temperature of the electro-thermal properties of the Peltier cells: the higher the temperature, the greater the value of the properties.

For our integrated air-water cooling system [5], the parameter $Q_{diss}$, the power dissipated through the walls of the equipment, plays a significant role, because in the design conditions the internal air temperature, $T_{a,i}$, is sensibly lower than the ambient one, $T_e$. The model proposed in Paragraph 2 has been thus used also to evaluate the behaviour of the cooling system for values of the operating room temperature, $T_e$, in the interval 0 ÷ +40°C [14]. The results of these calculations are shown in figure 6.

It is useful to begin the examination of figure 6 with the values of the power to be cooled in the finned heat sink, $Q_C$, and of that absorbed by the Peltier cells, $Q_{TEC}$. For a fixed value of $T_{a,i}$, when the ambient temperature decreases, the power to be cooled, $Q_C$, also decreases, and the reduction is significant. The lower cooling power requires a lower power absorbed by the Peltier cells, $Q_{TEC}$. The

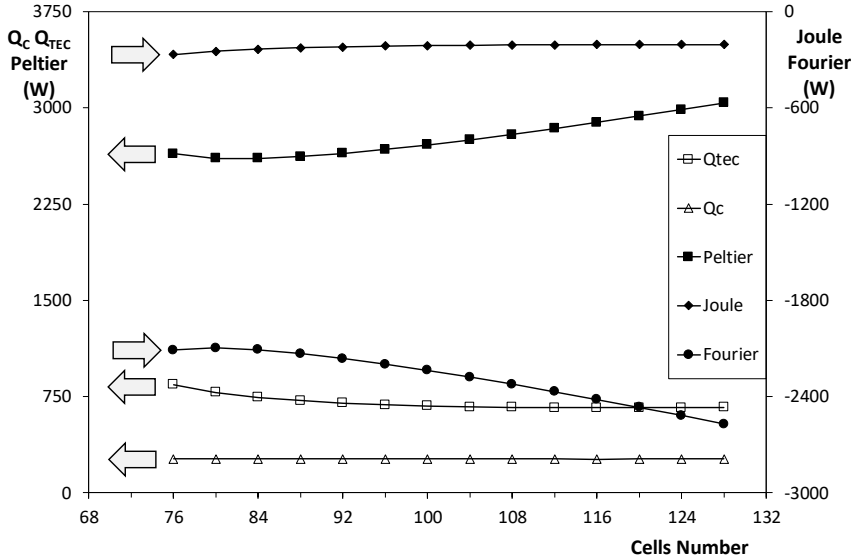


**Figure 4.** Trends of the different power terms of equation (7) as a function of the number of cells ($Q_{DL}$ = 5 kW).

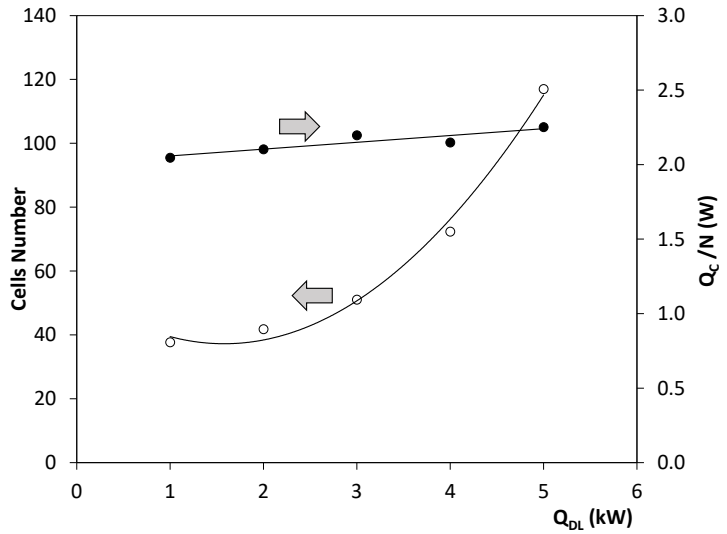


**Figure 5.** Number of cells for the "Maximum EER" and cooling power for single cell.

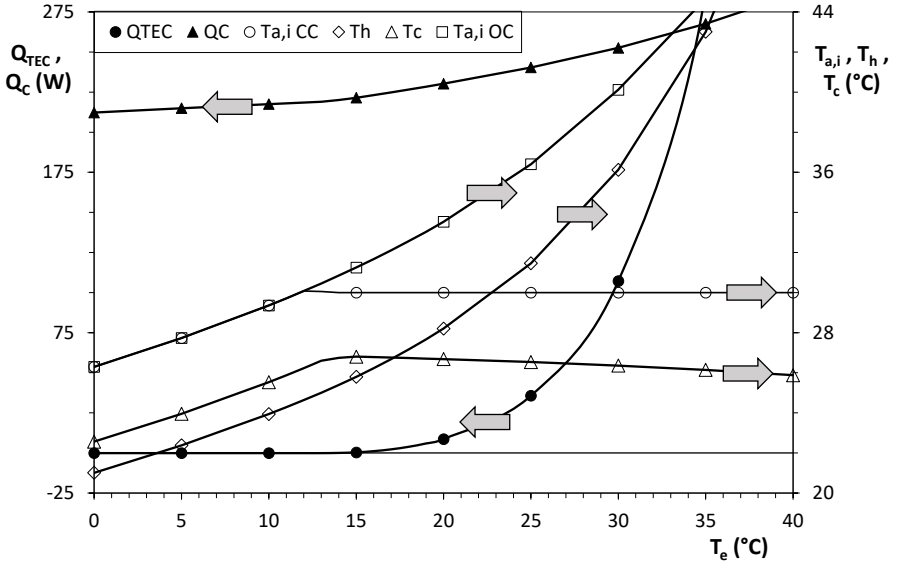


**Figure 6.** Different temperatures (white symbols) and heat fluxes (black symbols) as a function of the ambient temperature, $T_e$.

decrease of $Q_{TEC}$ is very strong in the interval +20°C < $T_e$ < +40°C.
In figure 6, beside the values of $Q_C$ and $Q_{TEC}$, the temperature is shown of the hot and cold junctions of the Peltier cells, $T_h$ and $T_c$ respectively, and the air temperature leaving the finned heat sink, $T_{a,i}$, both for closed and open circuit on the electrical load.
The fast decrease of $Q_{TEC}$ in the interval +20°C < $T_e$ < +40°C is matched to an also decreasing difference of temperature between the junctions of the Peltier cells, $T_h$ - $T_c$ . In more details, the hot junction temperature, $T_h$, shows a very fast decrease, while the cold junction temperature, $T_c$, is quite constant. This is true up to an ambient temperature, $T_e$, of 17°C, where the difference of temperature, $T_h$ - $T_c$, becomes zero. For $T_e$ < 17°C, the Peltier cells start working as an electricity generator. The power generated is generally small, depending on the thermal resistance of the connected power supply. For instance, for a typical switched power supply, the load resistance in "stand-by" condition (power ON and no power supplied) is about 1 Ω, while in "connected" condition (power OFF and connected) is about 1000 Ω.
For values of the ambient temperature lower than 17°C the temperature of the air leaving the finned heat sink, $T_{a,i}$, is still 30°C without any thermoelectric cooling contribution, since the Peltier cells are working as an electricity generator.
For values of the ambient temperature lower than 12°C, the temperature of the air leaving the finned heat sink, $T_{a,i}$, is even lower than 30°C, always without any need of a thermoelectric cooling contribution.
In the region of $T_e$ where the difference of temperature, $T_h$ - $T_c$, becomes negative and the thermoelectric power $Q_{TEC}$ is zero, the cooling power is exchanged with the cooling water by the "thermal" conduction through the Peltier cells. For this reason, for $T_e$ < 17°C the cold junction becomes hotter than the hot one ($T_c$ > $T_h$). In this region the thermoelectric cooler switches to a thermoelectric generator and at its ends a small voltage can be measured.
By comparing the distributions of temperature obtained for the power supply of the cells ON ($T_{a,i,CC}$) or disconnected ($T_{a,i,OC}$), in figure 6 the cooling effect of the Peltier cells is well evident. For low values of the ambient temperature ($T_e$ < 13°C) the two distributions are quite coincident. The limited difference is due to the fact the in the case of open circuit (power supply disconnected), the equivalent

electric resistance at its ends tends to infinity, while in the case of closed circuit (power supply connected even if switched OFF) the equivalent electric resistance is finite (about 1000 Ω).
For values of the ambient temperature higher than 13°C, when the power supply is disconnected, OC, the temperature of the air leaving the finned heat sink is soon so high to make the situation unsafe. Conversely, when the power supply is connected and switched ON, the thermoelectric cooler, when properly regulated, is able to maintain the required value $T_{a,i,CC}$ = 30°C.

## 4. Concluding remarks

A theoretical investigation is carried out of the thermal behaviour of a new cooling system [5] for high power electronics based on the combination of thermoelectric cooling, air-cooling and liquid cooling. A comprehensive numerical model, specifically tailored for this hybrid cooling system, is developed, based on a lumped parameter approach. The model is calibrated through an exhaustive comparison of numerical results versus experimental data, based on the data gathered in experiments already published [5].
With this model, the cooling system is analysed for working conditions different from those previously experimented [5], characterized by higher useful powers, which are consistent with manufacturer's new future operational conditions.
Useful information is obtained on the behaviour of the thermoelectric cooler (TEC), in particular on its optimum design.
The utilization of a TEC seems to be a proper solution if the ambient air temperature is as high as required by the Electronics Standards, because it is able to create an internal environment at the proper temperature. For a complete exploitation of the TEC, an accurate design of the system on the base of the parameters affecting its performance is required. Differently, the risk of a dissipation of power without a corresponding cooling effect exists. Finally, we can say that the proposed numerical model is the correct instrument for the design stage.

## 5. References

[1] Casano G and Piva S 2015 Air-water cooling system for switch-mode power supplies, *J. Electronics Cooling and Thermal Control* **5** 66–75
[2] Hirota M, Baba T, Zheng X, Nii K, Ohashi S, Ariyoshi T and Fujikawa H 2011 Development of new AC/DC converter for PHEVs and EVs, *SEI Technical Review* **73** 68-72
[3] Tani A and Camara M B 2013 DC/DC and DC/AC converters control for hybrid electric vehicles energy management - ultra capacitors and fuel cell, *IEEE Trans. on Industrial Informatics* **9** 686-696
[4] Oliveira J G, Schettino H, Gama V, Carvalho R and. Bernhoff H 2012 Implementation and control of an AC/DC/AC converter for double wound flywheel Application *Advances in Power Electronics* Article ID 604703 1-8
[5] Casano G and Piva S 2017 Experimental investigation of a Peltier cells cooling system for a Switch-Mode Power Supply *Microelectronics Reliability* **79** 426–432
[6] Gupta K, Da Silva C, Nasr M, Assadi A, Matsumoto H, Trescases O and Amon C H 2018 Thermal management strategies for a high-frequency, bi-directional, on-board electric vehicle charger, *17th IEEE ITHERM Conf.*, San Diego, CA, USA
[7] Morini G L, Piva S 2007 The simulation of transients in thermal plant. Part I: Mathematical model *Applied Thermal Engineering* **27** 2138–2144
[8] Morini G L, Piva S 2008 The simulation of transients in thermal plant. Part II: Applications *Applied Thermal Engineering* **28** 244-251
[9] Ferrandi C, Iorizzo F, Mameli M, Zinna S, Marengo M 2013 Lumped parameter model of sintered heat pipe: Transient numerical analysis and validation *Applied Thermal Engineering* **50** 1280-1290
[10] Carotenuto A, Casarosa C 2000 A lumped parameter model of the operating limits of one-well geothermal plant with down hole heat exchangers *Int. J. Heat Mass Transfer* **43** 2931-2948
[11] Boglietti A, Cavagnino A, Staton D, Shanel M, Mueller M, Mejuto C 2009 Evolution and

Modern Approaches for Thermal Analysis of Electrical Machines *IEEE Trans. on Industrial Electronics* **56** 871-882
[12] Kokalari I, Karaja T, Guerrisi M 2013 Review on lumped parameter method for modelling the blood flow in systemic arteries *J. Biomedical Science and Engineering* **6** 92-99
[13] Luo Z 2008. A simple method to estimate the physical characteristics of a thermoelectric cooler from vendor datasheets *Electronics Cooling* **14** 22-27
[14] European Telecommunication Standard 1995 ETS 300 384 Radio broadcasting systems; Very High Frequency (VHF), frequency modulated, sound broadcasting transmitters

**Nomenclature**

*Symbols*

| | | | |
|---|---|---|---|
| A | area ($m^2$) | N | number of Peltier cells |
| c | specific heat (J/kgK) | Q | heat flow (W) |
| EER | Energy Efficiency Ratio | $Q_v$ | flow rate ($m^3/s$) |
| I | electrical current (A) | R | thermal resistance ($KW^{-1}$) |
| K | overall heat transfer coefficient ($W/(m^2K)$) | $R_{el}$ | electrical resistance (Ω) |
| | | S | electromotive force (V/K) |
| (KS) | thermal transmittance ($WK^{-1}$) | T | temperature (°C) |
| L | thickness (m) | V | voltage (V) |

*Greek symbols*

| | |
|---|---|
| ρ | density ($kg/m^3$) |

*Subscrits*

| | | | |
|---|---|---|---|
| a | internal air | h | hot junction |
| c | cold junction | H | hot side of the TEC |
| C | at the base finned heat sink | i | inlet |
| CC | closed circuit | m | mean |
| cell | for a single cell | max | maximum |
| diss | power exchanged through the walls of the casing with the ambient | MOSFET | electronic active components |
| | | o | outlet |
| DL | dummy load, electric useful power | OC | open circuit |
| e | external ambient | pc | passive components |
| f | finned heat sink | TEC | thermoelectric cooler |
| fan | produced by the fans | w | water |